Thermal Behavior in a Solar Air Heater Channel with Ribs and Rectangular Winglets

Teerapat Chompookham[1], Ming Lokitsangtong[1], Smith Eiamsa-ard[2] and Pongjet Promvonge[1,*]

[1] Department of Mechanical Engineering, Faculty of Engineering, King Mongkut's Institute of Technology Ladkrabang, Bangkok 10520, Thailand

[2] Department of Mechanical Engineering, Faculty of Engineering, Mahanakorn University of Technology, Bangkok 10530, Thailand

*Corresponding Author: Tel: +662 329 8350-1, Fax: +662 329 8352,

E-mail: kppongje@kmitl.ac.th

Abstract

Effects of combined ribs and winglet-type vortex generators (WVG) on forced convection heat transfer and friction loss behaviors for turbulent airflow through a constant heat flux channel of solar air heater are experimentally investigated. Measurements are carried out in the channel of aspect ratio, AR = 10 and height, H = 30 mm. The cross-section of the rib placed only on the upper channel wall to create a reverse-flow is an isosceles triangle shape with a single rib height ratio, e/H = 0.2 and rib pitch ratio, P_r/H = 1.33. For WVG, ten pairs of rectangular winglets having a height, b/H = 0.4; transverse pitch ratio, P_t/H = 1; two different WVG arrangements by pointing upstream (PU) and pointing downstream (PD) of the flow and various attack angles (α) of 60°, 45° and 30° are mounted on the test duct entrance to generate longitudinal vortex flows through the tested channel. The flow rate is in terms of Reynolds numbers based on the inlet hydraulic diameter of the channel ranging from 5000 to 23,000. The experimental results show a significant effect of using the combined ribs and WVG on the heat transfer rate and friction loss over the smooth wall channel. The larger the attack angle leads to higher heat transfer and friction loss than the lower one and the PD-WVG provides higher heat transfer rate and friction loss than the PU one for similar operating conditions. In comparison, the largest attack angle of the PD-WVG yields the highest increase in Nusselt number and friction factor while the lowest attack angle of the PU-WVG gives the best thermal performance.

Keywords*:* enhanced heat transfer; rib; turbulent channel flow; vortex generator; winglet.

1. Introduction

In design of channel heat exchangers, rib, fin or baffle turbulators are often employed in order to increase the convective heat transfer rate leading to the compact heat exchanger and increasing the efficiency. For decades, ribs have been applied in high-performance thermal systems due to their high thermal loads. The cooling or heating air is supplied into the channels with several ribs to increase the stronger turbulence intensity of cooling or heating levels over the smooth wall channel. Ribs placed repeatedly in the channels interrupt hydrodynamic and thermal boundary layers because

downstream of each rib the flow separates, re-circulates, and impinges on the channel walls that are the main reasons for heat transfer enhancement in such channels. The use of ribs not only increases the heat transfer rate but also substantially the pressure loss. In particular, the rib geometry, the rib-to-channel height ratio and the rib pitch-to-height ratio are parameters that affect the heat transfer rate and the thermal performance. In general, the staggered rib with $e/H \approx 0.1$ and $P/H \approx 0.1$ is suggested in the literature. Winglets have been successfully used for enhancement of heat transfer of modern thermal systems because they can generate longitudinal vortex flow and help to destabilize the main flow with less penalty of pressure loss. Several investigations have been carried out to study the effect of parameters of wing turbulators on heat transfer and friction factor for two opposite roughened surfaces. There has been much interest in enhanced surfaces having punched winglet vortex generator [1-5]. These winglets were designed to generate longitudinal vortices which increase turbulence levels and improve convection resulting in improved heat transfer performance, albeit with a minimal pressure drop penalty. The vortices generated were a result of the introduction or exploitation of secondary flows, rather than the manipulation or alteration of the main flow.

The main aim of this work is to examine heat transfer and friction loss behaviors for airflow through a constant heat flux channel fitted with combined isosceles triangular ribs and rectangular winglets turbulators. Effects of WVG arrangements by pointing upstream (PU) and pointing downstream (PD) of the flow and effects of attack angle (α) on heat transfer and friction loss in the channel are experimentally investigated. Experimental results using air as the test fluid are presented in turbulent channel flows in a range of Reynolds number from 5000 to 23,000.

2. Experimental Setup

A schematic diagram of the experimental apparatus is presented in Fig. 1. In the figure, a circular pipe was used for connecting a high-pressure blower to a settling tank, which an orifice flow meter was mounted in this pipeline while a rectangular duct including a calm section and a test section was employed following the settling tank. The rectangular duct configuration was characterized by the channel height, H = 30 mm. The overall length of the channel was 2000 mm which included length of the test section, L = 440 mm with the channel width, W, of 300 mm. The rib dimensions are 6 mm high (e), 20 mm thick (t) and rib pitch, P_r = 40 mm. The form of ribbed plates was accomplished by means of wire-EDM (electrical discharge machine) machining. The ten pairs of rectangular winglets with the WVG height, b/H = 0.4 and transverse pitch, P_t = 30 mm was fabricated from 0.30 mm thick aluminum plates are mounted with various attack angles (α) of 60°, 45° and 30° on the tested duct entrance by using hot glue to create a longitudinal vortex flow over the tested channel as can be seen in Fig. 2.

The channel test section consisted of the two parallel walls as shown in Fig. 2. The AC power supply was the source of power for the plate-type heater, used for heating the upper plate of the test section only in order to maintain a uniform surface heat flux. A conducting

compound was applied to the heater and the principal upper wall to reduce contact resistance. Special wood bars, which have a much lower thermal conductivity than the metallic wall, were placed on the inlet and exit ends of the upper and lower walls to serve as a thermal barrier at the inlet and exit of the test section.

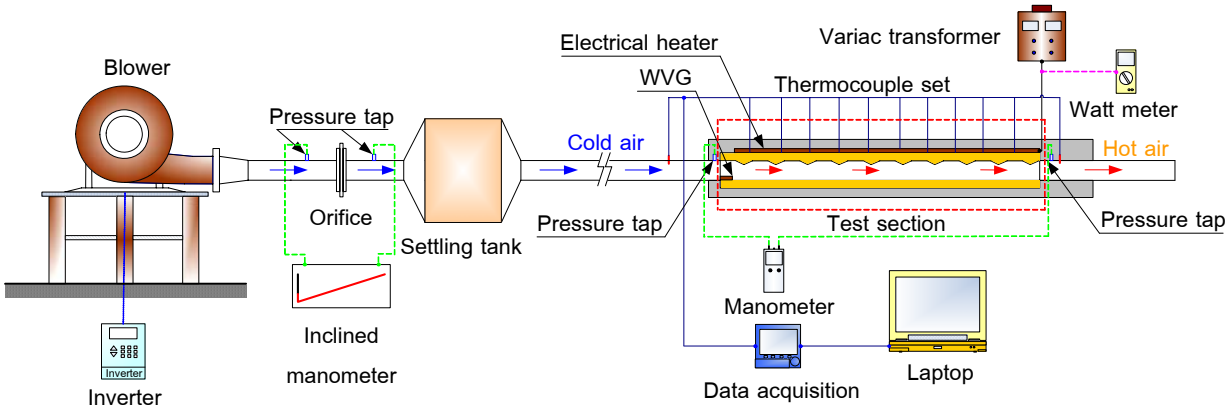

Fig. 1 Schematic diagram of experimental apparatus.

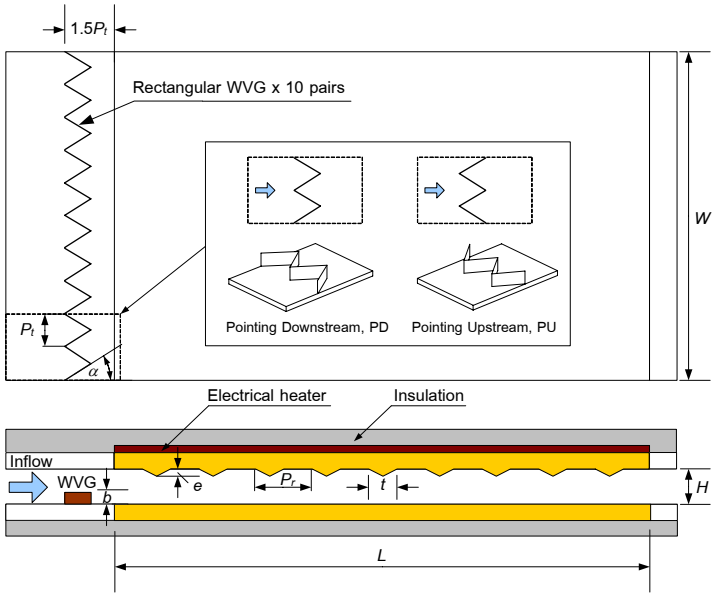

Fig. 2 Test section with PU and PD-WVG arrangements.

Air as the tested fluid in both the heat transfer and pressure drop experiments, was directed into the systems by a 1.45 kW high-pressure blower. The operating speed of the blower was varied by using an inverter to provide desired air flow rates. The flow rate of air in the systems was measured by an orifice plate pre-calibrated by using hot wire and vane-type anemometers (Testo 445). The pressure across the orifice was measured using inclined manometer. In order to measure temperature distributions on the principal upper wall, ten thermocouples were fitted to the wall. The thermocouples were installed in holes drilled from the rear face and centered of the walls with the respective junctions positioned within 2 mm of the inside wall and axial separation was 40 mm apart. To measure the inlet bulk temperature, two thermocouples were positioned upstream of duct inlet. All thermocouples were K type, 1.6 mm

diameter wire. The thermocouple voltage outputs were fed into a data acquisition system and then recorded via a personal computer.

Two static pressure taps were located at the top of the principal channel to measure axial pressure drops across the test section, used to evaluate average friction factor. These were located at the centre line of the channel. One of these taps is 50 mm upstream of the leading edge of the test channel and the other is 30 mm downstream of the test channel. The pressure drop was measured by a digital differential pressure connected to the 2 mm diameter taps.

To quantify the uncertainties of measurements the reduced data obtained experimentally were determined. The uncertainty in the data calculation was based on Ref. [6]. The maximum uncertainties of non-dimensional parameters were ±5% for Reynolds number, ±8% for Nusselt number and ±10% for friction. The uncertainty in the axial velocity measurement was estimated to be less than ±7%, and pressure has a corresponding estimated uncertainty of ±5%, whereas the uncertainty in temperature measurement at the channel wall was about ±0.5%.

3. Data Reduction

The goal of this experiment is to investigate the Nusselt number in the channel. The Reynolds number based on the channel hydraulic diameter, D_h, is given by

$$\mathrm{Re} = UD_h / \nu \,, \tag{1}$$

where U and ν are the mean air velocity of the channel and kinematics viscosity of air, respectively. The average heat transfer coefficient, h, is evaluated from the measured temperatures and heat inputs. With heat added uniformly to fluid (Q_{air}) and the temperature difference of wall and fluid (T_w-T_b), the average heat transfer coefficient will be evaluated from the experimental data via the following equations:

$$Q_{air} = Q_{conv} = \dot{m} C_p \left(T_o - T_i\right) = VI \,, \tag{2}$$

$$h = \frac{Q_{conv}}{A\left(\tilde{T}_s - T_b\right)}, \tag{3}$$

in which,

$$T_b = (T_o + T_i)/2 \,, \tag{4}$$

And

$$\tilde{T}_s = \sum T_s /10 \,. \tag{5}$$

The term A is the convective heat transfer area of the heated upper channel wall whereas $\tilde{T}_s$ is the average surface temperature obtained from local surface temperatures, T_s, along the axial length of the heated channel. The terms $\dot{m}$, C_p, V and I are the air mass flow rate, specific heat, voltage and current, respectively. Then, average Nusselt number, Nu, is written as:

$$\mathrm{Nu} = \frac{hD_h}{k} \,. \tag{6}$$

The friction factor, f, is evaluated by:

$$\mathrm{f} = \frac{2}{\left(L/D_h\right)} \frac{\Delta P}{\rho U^2}, \tag{7}$$

where ΔP is a pressure drop across the test section and ρ is density. All of thermo-physical properties of the air are determined at the overall bulk air temperature, T_b, from Eq. (4).

For equal pumping power,

$$\left(\dot{I}\Delta P\right)_0 = \left(\dot{I}\Delta P\right), \tag{8}$$

in which $\dot{I}$ is volumetric air flow rate and the relationship between friction and Reynolds number can be expressed as:

$$\left(\mathrm{f}\,\mathrm{Re}^3\right)_0 = \left(\mathrm{f}\,\mathrm{Re}^3\right),$$
$$\mathrm{Re}_0 = \mathrm{Re}\left(\mathrm{f}/\mathrm{f}_0\right)^{1/3} . \tag{9}$$

The thermal enhancement factor, η, defined as the ratio of heat transfer coefficient of an augmented surface, *h* to that of a smooth surface, h_0, at the same pumping power:

$$\eta = \left.\frac{h}{h_0}\right|_{pp} = \left.\frac{\mathrm{Nu}}{\mathrm{Nu}_0}\right|_{pp} = \left(\frac{\mathrm{Nu}}{\mathrm{Nu}_0}\right)\left(\frac{\mathrm{f}}{\mathrm{f}_0}\right)^{-1/3} . \quad (10)$$

4. Results and Discussion

In the present work, experimental measurements of both heat transfer and pressure loss in a channel fitted with an isosceles triangular rib (*e*/*H* = 0.2) and the rectangular WVG (*b*/*H* = 0.4) placed on the lower plate entrance with the attack angle, α = 60°, 45° and 30° with respect to axial flow direction are presented. Measurements were conducted in the channel of aspect ratio, AR = 10 for two arrangements and three attack angle values over a range of Reynolds numbers as mentioned earlier.

4.1 Verification of smooth channel

The present experimental results on heat transfer and friction characteristics in a smooth wall channel are first validated in terms of Nusselt number and friction factor. The Nusselt number and friction factor obtained from the present smooth channel are, respectively, compared with the correlations of Dittus-Boelter and Blasius found in the open literature [7] for turbulent flow in ducts.

Correlation of Dittus-Boelter,

$$\mathrm{Nu} = 0.023\,\mathrm{Re}^{0.8}\,\mathrm{Pr}^{0.4} \quad \text{for heating.} \quad (11)$$

Correlation of Blasius,

$$\mathrm{f} = 0.316\,\mathrm{Re}^{-0.25} \text{ for } 3000 \le \mathrm{Re} \le 20{,}000 . \quad (12)$$

Fig. 3a and b shows, respectively, a comparison of Nusselt number and friction factor obtained from the present work with those from correlations of Eqs. (9) and (10). In the figures, the present results agree very well within $\pm$6% for both friction factor and Nusselt number correlations.

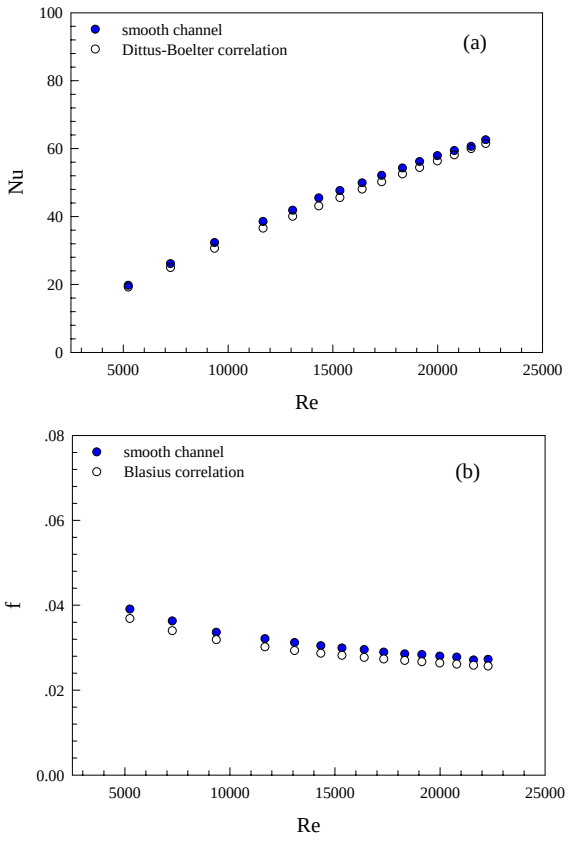

Fig. 3 Verification of (a) Nusselt number and (b) friction factor for smooth channel.

4.2 Effect of combined rib and WVG

The present experimental results on heat and flow friction characteristics in a uniform heat flux channel equipped with combined an isosceles triangular rib and the rectangular winglet turbulators are presented in the form of Nusselt number and friction factor. The Nusselt numbers obtained under turbulent flow conditions are presented in Fig. 4. In the figure, the combined rib and WVG yield the considerable heat transfer enhancements with a similar trend in comparison with the smooth channel and the Nusselt number increases with the rise of Reynolds number. This

is because the rib turbulators interrupt the development of the boundary layer of the fluid flow and create the reverse/recirculating flow behind the rib while the WVG pairs generate the longitudinal vortex flows that assist to wash up the reverse flow trapped behind the ribs into the core flow.

The effect of using the rib and WVG on the isothermal pressure drop across the tested channel is presented in Fig. 5. The variation of the pressure drop is shown in terms of friction factor with Reynolds number. In the figure, it is apparent that the use of the rib and WVG leads to a substantial increase in friction factor over the smooth channel.

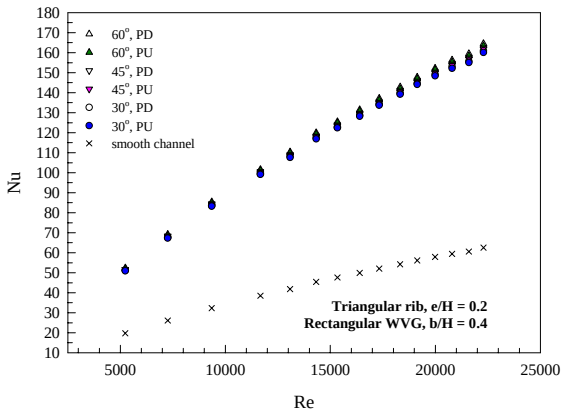

Fig. 4 Variation of Nusselt number with Reynolds number for various WVG.

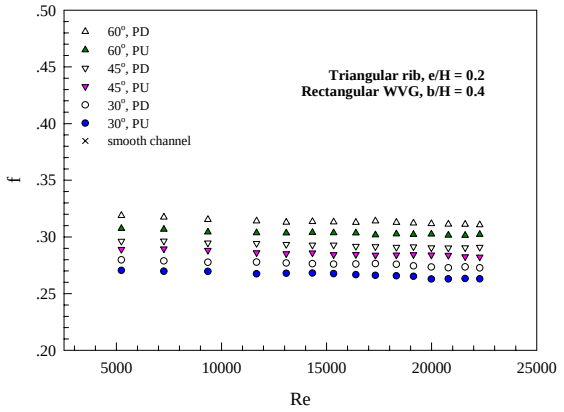

Fig. 5 Variation of friction factor with Reynolds number for various WVG.

4.3 Effect of WVG arrangement

The present results are reported for using two rectangular-WVG arrangements: pointing upstream (PU) and pointing downstream (PD) of the flow. Comparisons of the heat transfer and friction loss in the channel fitted with the PU and the PD-WVG in conjunction with the ribs are also depicted in Figs. 4 and 5, respectively. It is visible in Fig. 4 that along with the ribs, the PD-WVG provides higher heat transfer rate than that with the PU-WVG one for all Reynolds numbers. The heat transfer rates obtained from using the PD-WVG and the PU-WVG are around 256-266% and 255-257% over those from the smooth channel, respectively, depending on the Reynolds number interval.

The variation of isothermal friction factor value with Reynolds number for two different WVG arrangements is also depicted in Fig. 5. In the figure, the friction factor for the PD-WVG is found to be considerably higher than that for the PU-WVG one and tends to be nearly uniform with the increase of Reynolds number.

4.4 Effect of WVG attack angle

It is visible in Fig. 3 that the Nusselt number value increases with raising the attack angle. The higher attack angle provides higher heat transfer rate than that with the lower one. This can be attributed to the higher flow blockage of the rectangular-WVG with higher the attack angle by considering the projected area of the rectangular-WVG in flow direction. The heat transfer rates obtained from the combined ribs and WVG with α = 60°, 45° and 30° are, respectively, around 164%, 160% and 157% over the smooth channel for the PD-WVG and 162%, 158% and 155% for the PU-WVG as can be seen

in Fig. 6. In addition, the use of combined the ribs and WVG leads to a slight decrease of Nusselt number ratios for increasing Reynolds number.

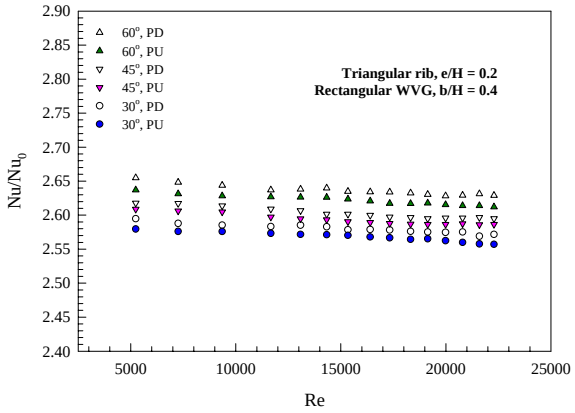

Fig. 6 Variation of Nusselt number ratio, Nu/Nu_0 with Reynolds number.

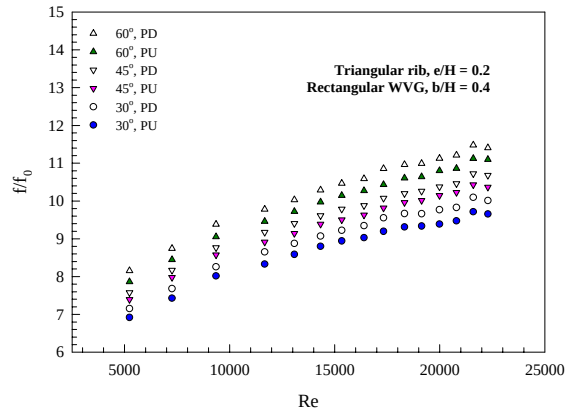

Fig. 7 Variation of friction factor ratio, f/f_0 with Reynolds number.

In Fig. 5, the friction factor value for the larger attack angle of the rectangular-WVG in conjunction with the ribs is found to be considerably higher than the lower one and tends to reduce slightly with the increase in Reynolds number. The increase in friction factor for the WVG is much larger than the smooth channel, especially for the case of α = 60°. The average increases in the friction factor for the WVG with α = 60°, 45° and 30° are, respectively, about 10.37, 9.68 and 9.12 times for PD-WVG and 10.03, 9.43 and 8.81 times for PU-WVG over the smooth channel as can be seen in Fig. 7.

4.5 Performance evaluation

The Nusselt number ratio, Nu/Nu_0, defined as a ratio of augmented Nusselt number to Nusselt number of smooth channel is plotted against the Reynolds number value as displayed in Fig. 6. In the figure, the Nusselt number ratio shows nearly constant values with the rise of Reynolds number.

Fig. 7 depicts the variation of the friction factor ratio, f/f_0, with the Reynolds number value. It is observed that the friction factor ratio tends to increase with increasing the Reynolds number for all WVG used. The increase in friction factor of the combined ribs and WVG is in a range of 6.29-11.48 times over the smooth channel, the PD-WVG provides a considerable increase in the friction factor ratio than that with the PU-WVG under the same conditions. This suggests that the use of the PU-WVG with the lower attack angle can help to reduce the pressure loss.

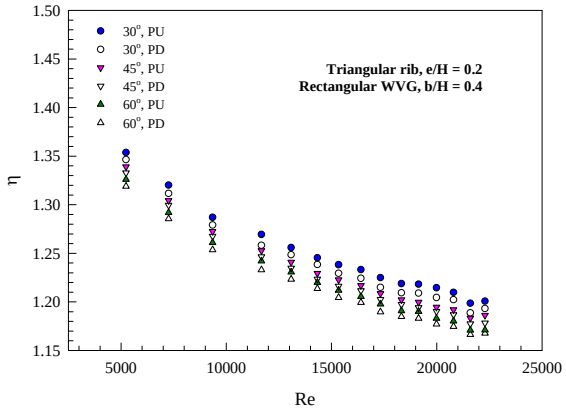

Fig. 8 Variation of thermal enhancement factor with Reynolds number.

Fig. 8 shows the variation of the thermal enhancement factor (η) with Reynolds number. The data obtained by the measured Nusselt number and friction factor values are compared at equal pumping power. It is seen in the figure that the enhancement factors (η) generally are above unity for using the ribs and the WVG. The

enhancement factor tends to decrease with the rise of Reynolds number values for all WVG. It is worth noting that the enhancement factor of the PU-WVG is higher than that of the PD-WVG for all Reynolds number values. The lowest attack angle (α = 30°) of the PU-WVG shows the best thermal enhancement factor of about 1.36 at the lowest value of Reynolds number.

5. Conclusion

An experiment has been carried out to investigate airflow friction and heat transfer characteristics in a high aspect ratio channel fitted with an isosceles triangular rib and the rectangular winglet type vortex generators (WVG) for the turbulent regime, Reynolds number from 5000 to 23,000. The use of the combined rib and WVG provides significantly higher heat transfer rate and friction loss than the smooth wall channel. The larger the attack angle value of the WVG leads to higher heat transfer rate and friction loss than the lower one. The PD-WVG performs higher heat transfer rate and friction loss than the PU one for similar operating conditions. In comparison, the largest attack angle (α = 60°) of the PD-WVG yields the highest increase in Nusselt number and friction factor while the lowest attack angle (α = 30°) of the PU-WVG shows the best thermal performance.

6. Acknowledgement

The funding of the work from the Thailand Research Fund (TRF) is gratefully appreciated.

7. References

[1] Lau, S, Meiritz, K, Vasanta Ram, VI. (1999). Measurement of momentum and heat transport in the turbulent channel flow with embedded longitudinal vortices, *International Journal of Heat and Fluid Flow*, vol. 20, pp. 128–141.

[2] Sohankar, A. (2007). Heat transfer augmentation in a rectangular channel with a vee-shaped vortex generators, *International Journal of Heat and Fluid Flow*, vol. 28, pp. 306–317.

[3] Li-Ting Tian, Ya-Ling He, Yong-Gang Lei, Wen-Quan Tao. (2009). Numerical study of fluid flow and heat transfer in a flat-plate channel with longitudinal vortex generators by applying field synergy principle analysis, *Int. Commun. Heat Mass Transf.,* vol. 36, pp. 111–120.

[4] Chompookham, T, Thianpong, C, Kwankaomeng, S, and Promvonge, P. (2010). Heat transfer augmentation in a wedge-ribbed channel using winglet vortex generators, *Int. Commun. Heat Mass Transf.*, vol. 37, pp. 163–169.

[5] Promvonge, P, Chompookham, T, Kwankaomeng, S, Thianpong, C. (2010). Enhanced heat transfer in a triangular ribbed channel with longitudinal vortex generators, *Energy Conversion and Management,* vol. 51, pp. 1242-1249.

[6] ANSI/ASME, (1986). *Measurement uncertainty*, PTC 19, 1-1985, Part I.

[7] Incropera, F., Dewitt, P.D. (2007). *Fundamentals of heat and mass transfer*, 6th edition, John Wiley & Sons Inc.